

Chlorosilane Production from Chlorine-Exposed Si(111) 7×7 and Cu/Si(111) SurfacesS. E. Sysoev,[†] D. V. Potapenko,[†] A. V. Ermakov,[†] B. J. Hinch,^{*,†} D. R. Strongin,[‡]
A. P. Wright,^{§,||} and C. Kuivila[⊥]*The Laboratory for Surface Modification and Department of Chemistry and Chemical Biology,
Rutgers University, Piscataway, New Jersey 08854, Department of Chemistry, Temple University,
Philadelphia, Pennsylvania 19122, Dow Corning Corporation, Midland, Michigan 48686,
and Dow Corning Corporation, Carrollton, Kentucky 41008**Received: September 7, 2001; In Final Form: December 12, 2001*

The adsorption of chlorine and desorption of chlorosilanes from chlorine-covered Si(111) and Cu/Si surfaces have been studied. The latter include annealed " 5×5 " Cu₂Si thin films as well as room-temperature deposited copper films on Si(111). Techniques employed include low-energy electron diffraction (LEED), Auger electron spectroscopy (AES), and temperature-programmed desorption (TPD). A Langmuir adsorption mechanism was observed for Cl on the Si(111) 7×7 surface, but a mobile precursor mediated process was observed for adsorption on the Cu/Si surfaces. Chlorine-exposed Si(111) 7×7 surfaces yield TPD peaks of SiCl₂ at ~ 650 °C with second-order desorption kinetics. For Cu-containing surfaces, similar TPD peaks were observed at slightly lower temperatures and with different desorption kinetics. The desorption rate includes a dependence on Cl-free sites. The presence of Cu on Si(111) also led to the appearance of two additional low-temperature TPD peaks, at 200 °C and 300 °C, both consisting of SiCl₄ and SiCl₂ species. We propose that the lower temperature desorption occurs through the formation of an activated SiCl₂ precursor on the copper-containing surface.

1. Introduction

In this paper we compare the reactions of Cl₂ on clean Si(111) 7×7 , on a well-defined Cu₂Si " 5×5 " film, and on Cu/Si alloy surfaces by means of Auger electron spectroscopy and thermal desorption under ultrahigh vacuum (UHV) conditions. The Cu/Si system is the basis of the so-called Direct Synthesis, or Rochow reaction used for the production of methylchlorosilanes in the modern silicone industry.¹ The Direct Synthesis, which uses methyl chloride as reactant, was extensively studied for more than half a century since its discovery. However, the molecular mechanisms operating in this reaction are unknown. The reason, in part, lies in undetectably low reaction rates of the Direct Synthesis under the UHV conditions required for application of the powerful surface science techniques now available.² Recently, however, it has been shown that it is possible to adsorb methyl radicals and chlorine sequentially on Cu/Si surfaces at low temperature in UHV. The adsorbed methyl and chlorine species interact with active Cu/Si sites to produce observable surface species that in TPD experiments desorb on warming to gaseous methylchlorosilanes, permitting application of the desired modern surface science techniques.^{3,4}

This paper presents studies into the chemistry of Cl₂, and production of chlorosilanes, on Cu/Si(111) surfaces. This work (with Cl adsorption alone) contributes to a fuller understanding of the active processes in the Direct Reaction. The Cu/Si(111) systems show different behavior to the Cu/Si(100) surfaces,

which have been the subject of earlier study.⁵ Most notably, at $T > 130$ °C deposited Cu atoms immediately condense within three-dimensional clusters leaving a large part of the Si(100) uncovered. In contrast, on Si(111) Cu will form a Cu₂Si film⁶ that is stable up to $T = 800$ °C. The Cu₂Si film or "quasi- 5×5 structure" has been studied extensively. It constitutes a monatomically thick incommensurate layer on the Si(111) surface, with a local two-dimensional stoichiometry of Cu₂Si. The proposed atomic structure is a hexagonal array of Cu and Si, where each Si atom is surrounded by six Cu atoms.^{7,8} On a larger scale, the nominally " 5×5 " LEED pattern indicates a well-defined discommensuration array in the Cu₂Si film. On Si(111) at room temperature, deposited Cu does not form a structure with a new periodicity; initially, the deposited Cu decorates the 7×7 structure. And in excess of a few monolayers, Cu films have been shown to grow epitaxially in a layer-by-layer mode.⁹

An Experimental Section, below, briefly describes both the apparatus used and calibration procedures employed in this work. We then present results of Cl₂ adsorption and chlorosilane production as observed on two characteristic surfaces: the Cu₂Si " 5×5 " film and a 10 ML thick Cu film, both on Si(111). Our results will also be compared to prior studies of Cl₂ chemistry on the atomically clean Si(111) 7×7 surface. Finally, we propose an atomic-scale mechanism that is consistent with our observations of chlorosilane desorption below 300 °C.

2. Experimental Section

The experiments were carried out in a UHV chamber with a base pressure of 2×10^{-10} Torr. A 4 grid LEED (Physical Electronics 11-020) system was used to observe electron diffraction patterns and to energy analyze Auger electron spectra. Temperature-programmed desorption (TPD) spectra were taken

* Author to whom correspondence should be addressed. Fax: (732) 445-5312. E-mail: jhinch@rutchem.rutgers.edu.

[†] Rutgers University.

[‡] Temple University.

[§] Dow Corning Corporation, Midland, MI 48686.

^{||} Present address: Strem Chemicals, Inc., Newburyport, MA 01985.

[⊥] Dow Corning Corporation, Carrollton, KY 41008.

with a quadrupole mass analyzer (UTI-100C); up to 4 ion masses could be monitored simultaneously.

The Si(111) samples (n-type, 0.05 Ω cm) were cut from wafer material supplied by Silicon Quest, Inc. The samples were typically outgassed for 30 min at 700 °C, their surface oxides were then removed at 1200 °C for up to 2 min, and the samples were subsequently cooled at rates as low as 1 K/s. After this treatment, the samples showed well-developed 7×7 reconstructions in the LEED patterns and impurities were not observable in AES spectra.

Well-controlled deposition fluxes of copper, at 0.3 ML/min, were achieved by evaporation and were monitored with a calibrated quartz microbalance. The copper coverages reported are measured in monolayers (ML) which are defined here as the density of sites on the Si(111) surface (taken as 7.84×10^{14} at./cm²).¹⁰ The Cu₂Si “ 5×5 ” surface was prepared by RT deposition of 3 ML of Cu onto a Si(111) 7×7 reconstructed substrate, and by subsequent annealing at 700 °C for 10 min. Sharp 5×5 LEED patterns were observed.

The Cl₂ doses were made using a solid-state AgCl electrochemical cell.¹¹ Before dosing, the cell was outgassed for approximately 10 h. During Cl dosing, the cell current was held constant at 20 μ A and the sample was placed in direct line-of-sight (at 8 cm) from the Cl source aperture. Background pressure in the experimental chamber did not rise during Cl₂ dosing.

The Auger spectra were measured using an electron beam (from the LEED gun) at a primary energy of 1.6 keV and a beam current of 5 μ A. For purposes of quantitative analyses, the relative peak-to-peak values of Si L_{2,3}VV (92 eV), Cu M_{2,3}-VV (60 eV), and Cl KVV (181 eV) transitions were determined. In what follows, we describe the procedure used to estimate chlorine coverages from AES spectra. It was assumed that all Cl atoms are surface bound and do not form bulk phases. This is consistent with the facts that bulk CuCl does not form as a result of Cl₂ adsorption on Cu(111) at temperatures above 0 °C¹² and that, for different clean Si faces, Cl₂ adsorption exhibited clear saturation.^{13–15} It was assumed also that the mean free path (escape depth) of the Auger electrons was comparable for both the Si and Cu lines. The surface concentration of chlorine was then estimated from¹⁶

$$\theta_{\text{Cl}} = \frac{\alpha I_{\text{Cl}}/\sigma_{\text{Cl}}}{I_{\text{Cu}}/\sigma_{\text{Cu}} + I_{\text{Si}}/\sigma_{\text{Si}} + I_{\text{Cl}}/\sigma_{\text{Cl}}}$$

where α is a normalization coefficient which would be a strong function of the Auger electron mean free path, I_X is the Auger peak-to-peak amplitude and σ_X is the Auger sensitivity factor for the element X. The precise sensitivity factors σ_X for the settings of our AES system are not readily available from the literature. Fortunately, the shape and time constant of the chlorine on Si(111) AES uptake curve (see Figure 1) is very insensitive to the $\sigma_{\text{Si}}/\sigma_{\text{Cl}}$ coefficient ratio. The chlorine on the Si(111) uptake curve, derived from TPD peak areas, must take the same shape (see the insert on the Figure 1). This is ensured by adopting $K = 0.4$ (a relative mass spectrometer sensitivity factor which is discussed below.) Relative values for $\sigma_{\text{Si}}/\sigma_{\text{Cl}}$ and $\sigma_{\text{Cu}}/\sigma_{\text{Cl}}$ were determined by making the TPD and AES saturation Cl uptake ratios consistent.

The *absolute* chlorine coverages to be reported here also depend on the normalization factor, α . (For Auger analysis of bulk phase concentrations α would be equated to 1. However, as we are concerned with Cl surface concentrations, a full layer of chlorine does not imply the absence of Si and/or Cu signals and α cannot equal 1.) α is obtained experimentally from the

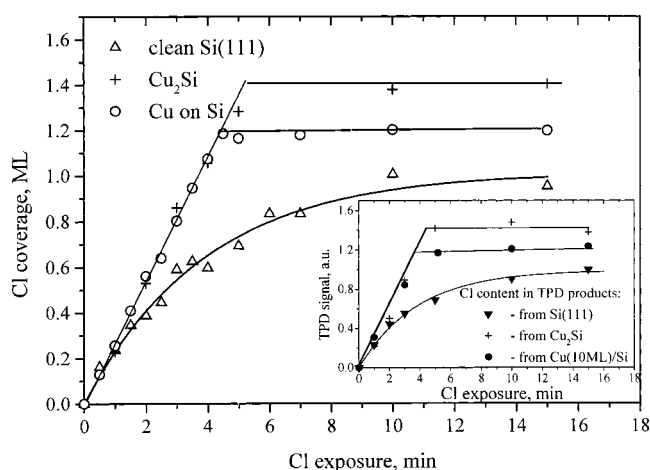


Figure 1. Normalized AES and TPD (insert) signals from different Si and Cu/Si surfaces as functions of chloride exposure.

Auger intensities from a Si(111) 7×7 surface that is subsequently annealed in chlorine at 450 °C for 15 min. Scanning tunneling microscopy (STM) studies have shown that under this treatment the surface forms a Cl-terminated (saturated) Si(111) 1×1 structure¹⁷ with a chlorine coverage, $\theta_{\text{Cl}} = 1$ ML.

Overall, the uncertainties of the σ_X ratios obtained give rise to approximately 10% errors in the *absolute* chlorine coverages for Cu-containing surfaces; however, the *relative* chlorine coverages for any particular surface are insensitive to the specific σ_X values. The shapes of the uptake curves are therefore reliable.

The surface temperature during TPD was measured by optical pyrometry. The pyrometer was calibrated in a prior experiment in which a thin chromel–alumel thermocouple had been melted into a Si sample. A heating rate of 20 °C/s was used for the TPD spectra.

Species that are prominent in the cracking patterns of the chlorosilanes (SiCl^+ , SiCl_2^+ , SiCl_3^+ , and SiCl_4^+) were monitored at m/e 63, 98, 133, and 170, respectively. To analyze the desorption product compositions, the mass spectrometer was calibrated first by backfilling the vacuum chamber with SiCl_4 . The ratios of signals for the different ions were $\{63\}:\{98\}:\{133\}:\{170\} = 0.7:0.12:1:0.34$. The cracking pattern of SiCl_2 was found from the mass analysis of the last TPD peak (around 600 °C). In all spectra that will be shown, the highest temperature peak originates solely from desorbing SiCl_2 . The ratio of the signals in these peaks was constant, $\{63\}:\{98\} = 2.6:1$, which is similar to ratios of 2.2 and 2.4 found in other studies of the electron-induced fragmentation of SiCl_2 .^{18,13} At other points in the TPD spectra, there can be other ratios of desorbing SiCl_4 and SiCl_2 . In the process described above, we have established the *relative* sensitivity, $K = k_{\text{SiCl}_2}^{63}/k_{\text{SiCl}_4}^{133} = 0.4 \pm 0.1$, where k_X^m is the sensitivity to the species X at the ion mass m . Each sensitivity is defined as the ratio of a TPD signal to the number of moles of molecules X desorbed from the sample. This sensitivity factor was checked in a series of experiments, where AES spectra were recorded after partial desorption of chlorosilanes and the calculated chlorine coverages were compared to integrated desorption peak areas. Using this *relative* sensitivity it was therefore possible to estimate the molecular compositions of the TPD products at any points in the TPD spectra.

In all our TPD spectra, obtained from different surfaces, the signals for masses 170 and 133 always followed the ratio of cracking products for SiCl_4 . In a similar way, after subtraction

of SiCl_4 signal contributions (for $m/e = 63$ and 98 amu) the ratio of remaining 63 and 98 signals always fitted to our cracking pattern of SiCl_2 . This implies that SiCl_2 and SiCl_4 were the only desorption products observed in our experiments, within an experimental uncertainty of ~ 0.05 ML of Cl.

It is necessary to mention here that SiCl_x^+ ions have the same masses as the ionization fragments of copper chlorides CuCl_{x-1}^+ . (The same masses are seen too for different Cl and Cu isotopes. The ratio for the common Cl isotopes, $\sim 3:1$ is discernibly different from the analogues for Cu, $\sim 2:1$.) The Cl-covered $\text{Cu}(100)$ surface has been shown to yield Cu_3Cl_3 at $T \sim 200$ °C and CuCl at $T \sim 600$ °C.^{19,20} Nevertheless we believe that, in our TPD experiments below 800 °C, immeasurably small amounts of Cu-containing products were formed, (a) as ions with mass 161 (Cu_2Cl^+) were never observed, (mass 161 is a major cracking fragment of Cu_3Cl_3 ¹⁹), and (b) as we did not observe any mass 98 signal that could not be attributed to the SiCl_4 and SiCl_2 products. (From the literature CuCl shows a much larger {98}: {63} ratio.)¹⁹ (c) Other supporting evidence comes from the fact that, for repeated TPD experiments below 800 °C from Cu_2Si films, we did not experimentally observe measurable reductions of Cu/Si AES intensity ratios. (d) Finally, our measurements of mass 63 to mass 65 yield ratios, r , lie in a range from 2.86 to 3.22, i.e., $r = 3.0 \pm 0.2$.

3. Results and Discussion

3.1. AES Experiments. For room-temperature deposition of copper on the $\text{Si}(111) 7 \times 7$ surface, an AES Si feature remains observable for copper coverages in excess of 100 ML. This could be anticipated from the high Cu–Si interdiffusion reported in the literature.¹⁰ (Si forms a solid solution in copper (Si < 10%) even at room temperature.) From the TPD data, to be presented below, we believe that our standard $\text{Cu}(10 \text{ ML})/\text{Si}$ overlayer exhibits a substantial Si surface concentration. STM data, not presented here, also indicate that at room temperature the copper film wets the Si surface, and has a minimal surface roughness.

AES evidence of chlorine uptake on the $\text{Si}(111) 7 \times 7$, $\text{Cu}_2\text{Si} 5 \times 5$, and $\text{Cu}(10 \text{ ML})/\text{Si}(111)$ surfaces is illustrated in Figure 1. In these experiments the sample was exposed to the chlorine flux for certain time intervals and AES spectra were recorded after each exposure. The relative chlorine coverages for each surface were calculated from the Cu, Si, and Cl Auger peak heights as described in the Experimental Section above.

In the case of the $\text{Si}(111) 7 \times 7$ surface, the relative chlorine coverage can be well approximated by an exponential curve as shown in Figure 1. A chlorine sticking probability that decreases linearly with increasing coverage is implied, consistent with simple Langmuir adsorption kinetics.²¹ We find also an absolute saturation coverage of a 7×7 surface at $\theta_{\text{Cl}} = 1.0 \pm 0.1$ ML which is supportive of values reported elsewhere, ~ 1 ML^{13,22} although is inconsistent with another reported value, 1.89 ML.¹⁴

The two Cu-containing surfaces, however, exhibit quite different adsorption kinetics (Figure 1). On these two surfaces the chlorine coverage increases almost linearly with exposure up to a point at which the uptake rate drops to essentially zero. The curve for the $\text{Cu}(10 \text{ ML})/\text{Si}$ surface has an especially pronounced kink at 4 min exposure. The shape of such an uptake curve corresponds to a constant sticking probability over a wide range of coverages. This behavior is typical for a precursor-mediated adsorption process.²¹ The $\text{Cu}(10 \text{ ML})/\text{Si}$ surface has the uptake curve shape that is indistinguishable from one observed for $\text{Cu}(111)$.²³ The uptake curve for Cu_2Si film also has an initial linear portion but the kink at about 4 min exposure

is not as well expressed. We propose that this may be due to the relatively high Si surface content and that surface Si can bind strongly to Cl. At high Si coverages the surface mobility of a Cl adsorption precursor may be substantially decreased.

Our hypothesis, that chlorine is bound preferentially to silicon on the Cu_2Si surface, would be supported by the fact that a Si–Cl bond energy at ~ 105 kcal/mol is greater than that for Cu–Cl bonds, ~ 84 kcal/mol.²⁴ A larger proportion of Cl on Si binding, to Cl on Cu binding, is also implied by our observation that the Si/Cu Auger signal ratio decreased (from ~ 3 at zero Cl coverage to ~ 1 at Cl saturation), indicating the preferential screening of Si atoms by the adsorbed chlorine.

The absolute chlorine coverage of $\text{Cu}(10 \text{ ML})/\text{Si}$ surface did not exceed 1.2 ± 0.2 ML in our measurements. This Cl coverage can be compared with 0.99 ML and 1.1 ML coverages, for, respectively, $\text{Cu}(111)$ and $\text{Cu}(100)$ surfaces,²³ which can be obtained before the onset of bulk chlorination. (Here, and throughout the paper, the absolute coverages are expressed in units of monolayers on $\text{Si}(111)$, i.e., $1 \text{ ML} \equiv 7.84 \times 10^{-14} \text{ cm}^{-2}$). The highest observed coverage for Cu_2Si is larger at 1.4 ML. The values of 1.2 and 1.4 ML must be explained by invoking a greater Cl packing density on copper in the presence of silicon than can be obtained on pure (Si-free) copper. The local surface density of Si in the Cu_2Si film is approximately 0.8 ML. If 3/4 of these Si atoms are doubly chlorinated, the total Cl coverage of 1.4 ML is achieved. Alternatively, a lesser fraction of Si could be doubly chlorinated and some more chlorine could be bound directly above copper. 1.2 ML of Cl is achievable on the 10 ML $\text{Cu}/\text{Si}(111)$ surface. From this fact we must conclude that some doubly chlorinated silicon species are contributing to the high Cl coverage, and Si atoms are present at the external interface. Again, this is supportive of Si diffusion through the copper film and segregation to the surface.

3.2. TPD Experiments. After the application of the $K = 0.4$ sensitivity factor, mentioned above, each of the uptake curves derived from integrated TPD spectra (see Figure 1) of Cl-containing species show very comparable shapes to those from the AES scans. This is fully consistent with a mobile precursor in the Cl_2 on $\text{Cu}(10 \text{ ML})/\text{Si}$ system and a precursor with reduced mobility in the Cl_2 on Cu_2Si adsorption system.

A typical TPD spectrum from a chlorine-saturated $\text{Si}(111) 7 \times 7$ surface is shown in Figure 2a. The desorption of SiCl_2 occurs in the range $T \sim 300$ – 500 °C followed by an intense peak at $T \sim 650$ °C. This spectrum is similar to other published results of thermal desorption from $\text{Si}(111) 7 \times 7$ surfaces saturated with molecular chlorine. In some studies a major desorption peak of SiCl_2 was observed between 600 and 720 °C.^{13,14,22} A minor SiCl_2 peak occurring between 420 and 500 °C has been associated with the adatoms on the 7×7 reconstruction.^{13,22,25} In the same scans, we have observed SiCl_4 desorbing in a very weak but broad peak extending from 200 to 500 °C. The low-temperature feature may arise from defects at the surface. While the necessary defect density could prevail as defects intrinsic to our 7×7 structures, it is also possible that the defects are introduced by exposure to atomic chlorine. In reference 14, as in our experiments, the electrochemical Cl_2 source was also used and a wide TPD feature between 150 and 400 °C consisting of both SiCl_2 and SiCl_4 was observed. (The resolution of their spectrum was too low to separate peaks in this temperature region.) An output of reactive atomic chlorine¹¹ and/or vibrationally excited molecular chlorine could lead to the formation of more highly chlorinated surface species and weak lower-temperature TPD peaks.

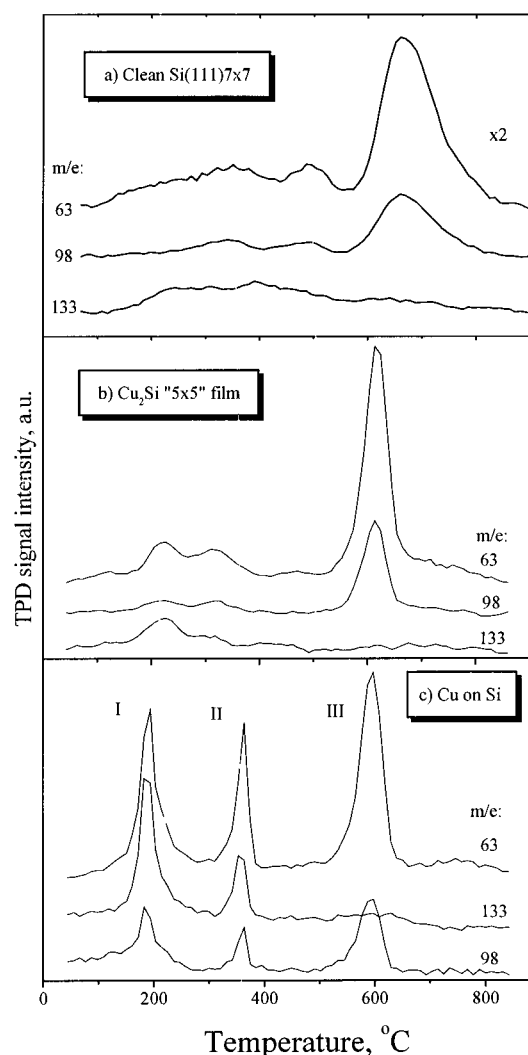


Figure 2. TPD mass spectra from (a) Si(111) 7×7 , (b) Cu_2Si “ 5×5 ”, and (c) Cu (10 ML) on Si(111) surfaces saturated with chlorine. Ions monitored: SiCl^+ ($m/e = 63$), SiCl_2^+ (98), and SiCl_3^+ (133).

For further discussion we shall refer to the three desorption peaks from our Cu-containing surfaces as peak I, II, and III (respectively, with increasing desorption temperature). Figure 2b shows a representative TPD spectrum from the Cu_2Si “ 5×5 ” film saturated with chlorine. The main peak (III) of SiCl_2 appears at 600°C which is 50°C lower than for the Si(111) 7×7 surface. This peak is also significantly narrower although it has approximately the same area as in the case of Si(111) 7×7 . The lower temperature peaks (I and II) are also shifted toward still lower temperatures: peak I is at approximately 210°C , and peak II is at 320°C . As peaks I and II overlap, the analysis of their composition is more difficult. It is possible to say though that peak I is predominantly SiCl_4 and peak II is composed of comparable amounts of SiCl_2 and SiCl_4 .

TPD experiments were also performed with approximately 10 ML of Cu on Si(111) 7×7 with chlorine saturation; the typical spectrum obtained is shown in Figure 2c. This spectrum has three peaks apparently of the same nature as the peaks on Cu_2Si surface—all three have approximately the same respective temperatures and composition of desorbing products. Peaks I and II, however, are more intense and are well separated, thereby allowing a reliable composition analysis. Peak I consists of $80 \pm 10 \text{ mol } \%$ of SiCl_4 , and peak II consists of $50 \pm 10 \text{ mol } \%$ of SiCl_4 , the remainder being SiCl_2 .

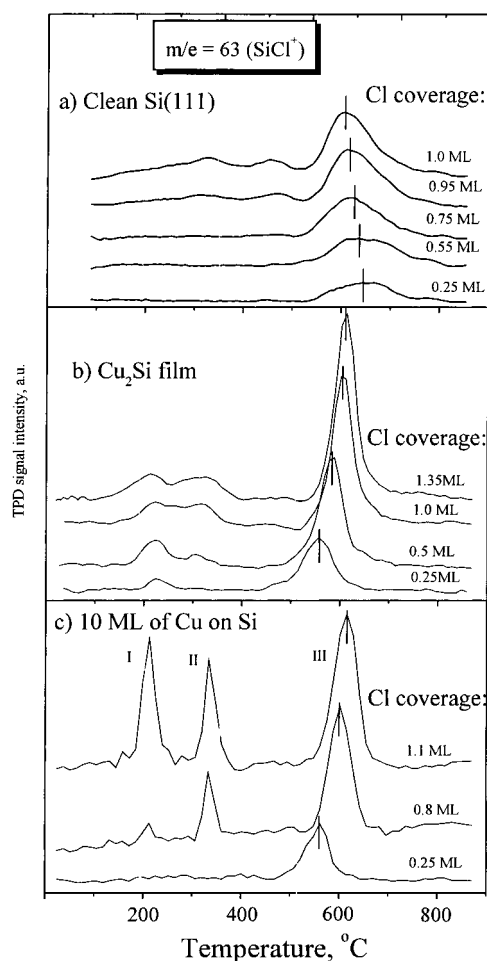


Figure 3. TPD spectra for different chlorine coverages from (a) clean Si(111) 7×7 , (b) Cu_2Si film, and (c) Cu (10 ML) on Si(111) 7×7 . Only the signal for SiCl^+ is shown.

It is evident from the TPD data of Figure 2c that a minimum of $\sim 0.15 \text{ ML}$ Si must be present at the surface of the Cu(10 ML)/Si overlayer at $\sim 200^\circ\text{C}$, and that as much as $\sim 0.55 \text{ ML}$ must have been accessible to the Cl for further chlorosilane desorption at temperatures up to 600°C . A restructuring and/or surface segregation must be present to account for the high silane TPD yields.

Above 800°C , both Cu-containing surfaces produce the desorption peak seen at mass 63 only. This is caused by the evaporation of Cu, and is supported by the presence of the same peak in TPD spectra from Cu/Si(111) (in the absence of adsorbed chlorine). Similar Cu desorption at about 700°C was observed from Cu/Si(100).⁵ The copper desorption peak is deliberately not shown in Figures 2b and 2c for clarity. The desorption temperature (800°C) was seemingly sufficient to desorb all of the Cu atoms, and/or drive the copper subsurface, because thereafter evidence for a surface copper concentration was not found in either AES or LEED.

The initial chlorine coverage dependence of the TPD spectra (Figure 3) reveals more details of the adsorption/desorption and Si etching chemistry on the studied surfaces. In the case of the clean Si(111) 7×7 surface (Figure 3a) the high-temperature SiCl_2 desorption peak shifts to lower temperature with increasing chlorine coverage, which is commonly taken as an indication of second-order desorption kinetics.^{13,22,26,27} The lower temperature peaks become noticeable only at $\theta_{\text{Cl}} > 0.8 \text{ ML}$. In ref 13, the lower temperature peak was observed for an initial coverage

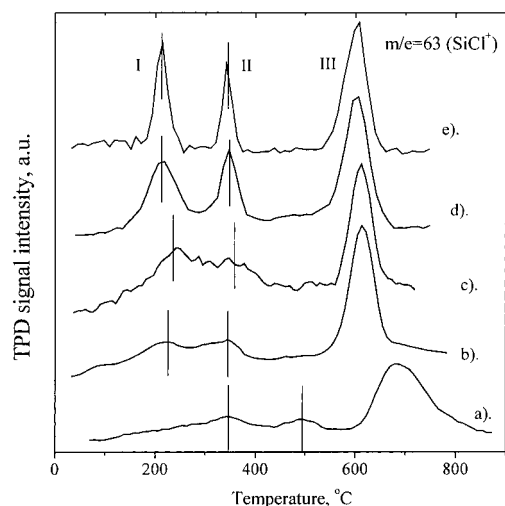


Figure 4. TPD mass spectra from Cl-saturated surfaces with different amounts of Cu: (a) clean Si(111) 7×7 , (b) Cu_2Si ; Cu/Si surfaces with (c) 2.5 ML, (d) 5 ML, and (e) 10 ML of Cu.

>0.6 of the chlorine saturation coverage—again consistent with our results.

In the case of the Cu/Si surfaces (Figures 3b and 3c) the main SiCl_2 peak (III) has a lower desorption temperature, it becomes narrower and shifts to higher temperatures with increasing chlorine coverage. Further analysis of this desorption process will be given in the following section.

An important observation about the lower temperature peaks can be made in Figure 3c. With increasing chlorine coverage the desorption peaks saturate consecutively in order III, II, I. This result implies that at the onset temperature of peak I (i.e., by $\sim 150^\circ\text{C}$) a fraction of the adsorbed chlorine is already in configurations that will, at higher temperatures, give rise to the peaks II and III.

A set of experiments were performed to test the interrelation of different desorption peaks from Cu/Si surfaces. First, the chlorine-saturated Cu(10 ML)/Si surface was ramped to 270°C (such that only peak I was observed) and cooled to room temperature. After 15 min, the sample was heated to 450°C and only the second desorption peak (II) was observed at $T \sim 320^\circ\text{C}$ without any traces of peak I. Then, after cooling back to RT, the sample was reheated and only peak III at $T \sim 600^\circ\text{C}$ was observed. Second, the chlorine-saturated Cu(10 ML)/Si surface was heated to 270°C (only desorption peak I was observed,) then cooled and reexposed to a further ~ 2 L of Cl_2 from the chlorine source. In the subsequent TPD experiment all three desorption peaks were observed. Collectively, these results imply that peak I does not correspond to the irreversible depletion of a specific type of silicon atoms (e.g., from special sites). The Cl/Si configurations that give rise to peak I can be replenished by additional chlorine exposure. Also, such replenishment does not occur by an unaided redistribution of chlorines and silicons that otherwise give rise to peaks II and III.

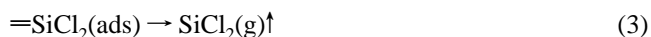
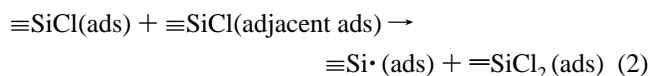
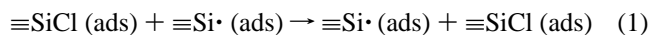
Finally, we have analyzed the copper coverage dependence of chlorosilane thermal desorption. Curves (c) through (e) of Figure 4 show TPD spectra from the Cl-saturated silicon surfaces with different amounts of copper (2.5–10 ML). Curves (a) and (b) of Figure 4 are the TPD spectra from the clean Si(111) 7×7 and the Cu_2Si surfaces, respectively, and are shown for reference. It can be seen, from these results, that peaks I and II become narrower with the increasing copper coverage but the areas of these peaks do not change significantly. Peak III is unaffected by the initial Cu concentration.

3.3. Discussion of Possible Desorption Mechanisms. We shall discuss the nature of desorption peaks in order of their consecutive appearance in TPD spectra with increasing chlorine coverages starting with the high-temperature desorption peak, i.e., peak III, which saturates first (see Figures 2 and 3).

The high-temperature SiCl_2 desorption peak from the chlorine-exposed Si(111) 7×7 surface shifted to lower temperatures with increasing chlorine coverage, as may be anticipated for a second-order desorption process for SiCl_2 .^{13,22,26,27} In addition, we have analyzed the high-temperature peaks using a differential approach²⁸ based on Redhead's method,²⁹ thereby establishing an independent estimate of the reaction order, n . We have constructed Arrhenius plots $\ln[(-d\theta/dT)/\theta^n(T)]$ vs $1/T$, where $(-d\theta/dT)$ is the desorption rate, and $\theta(T)$ is the chlorine coverage at temperature T . The values of $(-d\theta/dT)$ were calculated by normalizing the intensity of mass 63 TPD signal. $\theta(T)$ was obtained by integrating the TPD peak to the right from temperature T and normalizing to the total peak area at the saturation coverage. The best n values were determined by preparing these Arrhenius plots for each TPD peak separately and by minimizing the mean square error of a linear fit to the experimental data. All n values lie between 1.7 and 2.2, supportive of other studies^{30,13} which state $n = 2$ for the desorption of SiCl_2 from Si(111) near 650°C .

Arrhenius plots with $n = 2$ are shown in Figure 5a. The data points for the TPD experiments with different initial coverages lie quite close to one another, which demonstrates that the kinetic parameters are initial-coverage independent. From this plot we obtained the activation energy $E_a = 52 \pm 4$ kcal/mol and the pre-exponential factor $\nu = 10^{12 \pm 1} \text{ s}^{-1}$. The quoted uncertainties come from the independent calculations for different initial chlorine exposures. Our value of $E_a = 52$ kcal/mol is lower than 71–67 kcal/mol^{18,13} and 83 kcal/mol³⁰ reported for Si(111), but is closer to 47 kcal/mol found for the desorption of SiCl_2 from Si(100).²⁶

According to XPS studies²⁷ on a chlorinated Si(111) surface annealed at 400°C virtually all chlorine is bound in monochloride species, $\equiv\text{SiCl}(\text{ads})$. Using this notation, \equiv and $=$ symbols refer to three and two Si–Si back-bonds into the surface. From our TPD spectra from chlorine saturated Si(111) 7×7 , we can estimate that at 450°C a small fraction of the surface silicon atoms (0.2 ML) is unsaturated, $\equiv\text{Si}\cdot(\text{ads})$. In general, the desorption of SiCl_2 near 650°C should proceed then according to the following equations:



Equation 1 represents the process necessary for Cl mobility. At 650°C and above, this process must be facile. Step (1) cannot be rate determining, as this would imply first-order desorption kinetics. Also, if (1) were rate limiting, (2) and (3) could proceed at temperatures below 650°C , until no more $\equiv\text{SiCl}(\text{adjacent ads})$ species exist. That would correspond to a minimum of 2/3 ML coverage of unsaturated $\equiv\text{Si}\cdot(\text{ads})$ species, at 600°C which is contrary to our observations. It is generally assumed that either the second or the third equations in this mechanism are rate limiting, as either would give rise to the observed second-order desorption kinetics.

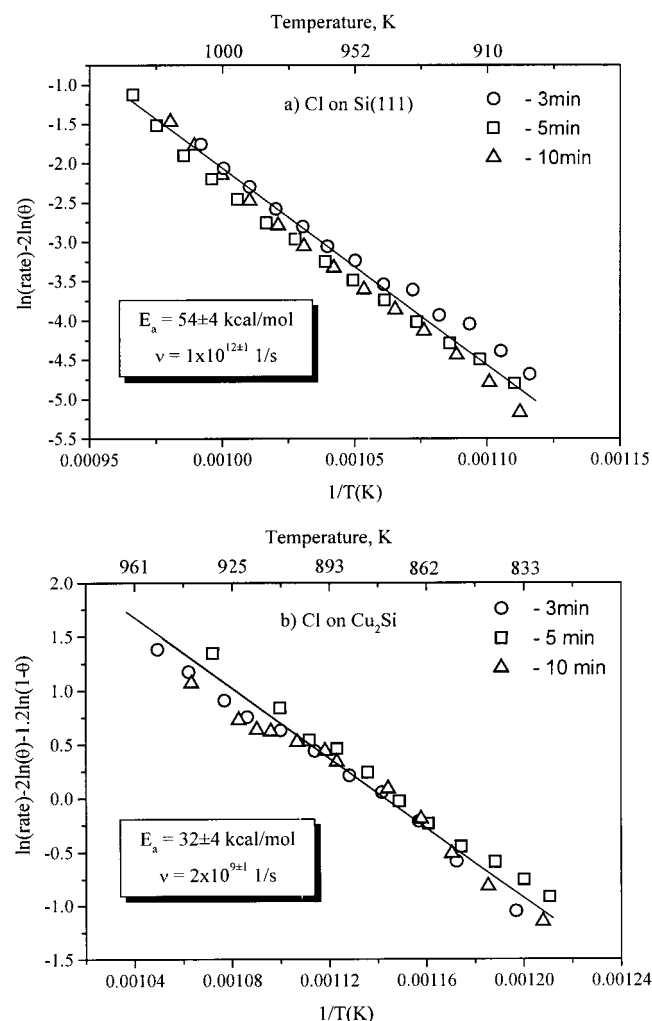


Figure 5. Arrhenius plots of the SiCl₂ desorption rate obtained from desorption spectra Figures 2a,b from (a) Cl on clean Si (7 × 7) and (b) Cl on Cu₂Si thin film at different initial Cl coverages. These plots are discussed further in the text.

Unlike clean silicon, the Cu-containing surfaces exhibited a more surprising dependence of desorption kinetics on chlorine coverage (Figures 3b and 3c). The III desorption peaks shift to higher temperatures as the initial Cl coverage increases. We have analyzed the III peaks from the Cu/Si surfaces using the same differential method as above. Kinetics of the type θ^n could not simultaneously explain both the shape and the shift of the peaks with initial coverage. Therefore we have employed $\theta^n(1 - \theta)^m$ as a preexponential function in the kinetic equation. This functional form was also used successfully to explain a similar peak temperature behavior in the study of SiCl₂ desorption from Si(100).²⁶ (N.B., the high-temperature peak is again believed to be saturated at 1.0 ML of Cl.) We found best values for the reaction orders $n = 2$ and $m = 1.2$ by minimizing R^2 in the Arrhenius plots $\ln[(-d\theta/dT)/\theta^n(1 - \theta)^m]$ vs $1/T$ (Figure 5b). The best kinetic parameters obtained from the plots are $E_a = 32 \pm 4$ kcal/mol and $\nu = 10^{9\pm1}$ s⁻¹.

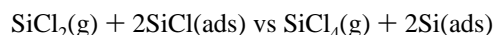
Peak III has approximately the same desorption temperature as the higher temperature peak from the clean Si(111). Also, in both cases, SiCl₂ is the only desorbing product and this peak is the first to appear with increasing Cl coverages. These observations would suggest that peak III is very similar in nature to the SiCl₂ peak from the Si(111) surface. Yet, copper substantially reduces the activation energy and also the apparent reaction pre-exponential term. The presence of the $(1 - \theta)$ term in the

kinetic equation might indicate the participation of chlorine-free surface sites in the SiCl₂ desorption process. Because of the undetermined mixed stoichiometry of the surface, we are not able to specify if the Cl-free sites refer to local copper or silicon sites.

A kinetic analysis of the lower temperature peaks, from the copper-containing surfaces, was not attempted because of poor reliability of temperature measurements in the $T < 300$ °C region. However, we propose some features of the desorption mechanisms for peak I and peak II that would still be consistent with our other experimental data.

Two desorption products, namely SiCl₂(g) and SiCl₄(g), are simultaneously present in each of the lower temperature desorption peaks. First, we propose that both desorption products are formed from the same surface intermediate X. Second, the rate of formation of this intermediate X controls the appearance of peaks I and II. Two different pathways, at temperatures ~200 and ~300 °C, must be activated to ensure the onset of peaks I and II, i.e., the formation of X must be rate determining in each of the peaks.

The different composition of the desorption products at peaks I and II could be determined by different activation enthalpies for SiCl_{2,4} formation from X alone. The observed SiCl₄/SiCl₂ ratios of 4 at peak I and 1 at peak II, separated by 100 K, would correspond to an activation enthalpy difference of 8 kcal/mol—SiCl₂ formation having a larger barrier than SiCl₄. This is not inconsistent with a simple consideration of heats of formation of a set of reactants and products. By considering two molecular arrangements:



by using the tabulated enthalpies of formation of SiCl_{2,4} and Cl,³¹ and by assuming the cited strength of a Cl—Si bond on the surface of 81 kcal/mol,³² we would deduce a difference of 14 kcal/mol in favor of SiCl₄ formation.

First let us consider the species present at the surface. The Cl uptake curves suggest that 1.4 ML of Cl is present on the Cu₂Si surface at the onset of peak I. Before peak I, the surface of the sample has SiCl(ads) and some undetermined balance of SiCl₂(ads) and CuCl(ads) surface species. It would not be necessary to invoke a long-lived SiCl₃(ads) species to account for the adsorbed chlorine density. At the conclusion of peak II, (if we accept the similarities in the desorption mechanisms above 400 °C from the clean silicon and copper-containing surfaces) all dichloride species are depleted, chlorine is not above the copper, silicon monochlorides predominate, and some chlorine-free silicons are present. Any proposed model must be consistent with these observations.

It is not possible to identify unambiguously the intermediate X from our data. Although we consider a SiCl₃(ads) species to be a necessary intermediate in SiCl₄ formation, we do not consider this a likely candidate for our intermediate X as it is not clear how SiCl₃(ads) can give rise to the SiCl₂(g) product directly. With consideration of other (simple) possibilities, we find we can be most strongly supportive of a model where X is a surface-bound activated species, SiCl₂*. Certainly, some SiCl₂ species must be present as an intermediate to SiCl₂ desorption from the SiCl₂(ads) surface state. The contrary, namely that SiCl₂ can desorb directly from a SiCl₂(ads) state (even at 200 °C, I), would imply that all SiCl₂(ads) species would be depleted by the end of peak I, which is inconsistent with our observations.

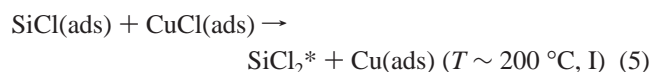
In our model we are therefore considering two types of SiCl₂ on the surface. The one, SiCl₂(ads), is produced by the double chlorination of a Si atom in the Cu/Si plane. The silicon atom

of $\text{SiCl}_2(\text{ads})$ is believed to be surrounded by 6 Cu atoms (see Cu_2Si “ 5×5 ” structure)⁷ and also is weakly bound to the second atomic layer beneath. This $\text{SiCl}_2(\text{ads})$ species is already present on the surface at the onset of peak I. In contrast, the SiCl_2^* could sit on top of the Cu/Si surface and the silicon atom could have as few as 3 adjacent Cu/Si atoms, to which it can bind.

Apparently, to produce SiCl_2^* from $\text{SiCl}_2(\text{ads})$ it is necessary to break a number of Si–Cu and/or Si–Si bonds. And SiCl_2^* has a limited coordination to the surface. An energetic barrier between the two SiCl_2 states is implied. We propose that the onset of peak II is determined by thermal activation of the $\text{SiCl}_2(\text{ads})$ species:



The second pathway for SiCl_2^* production, responsible for peak I, could be the following process:



Note: here we have dropped the “ \equiv ” and “ $=$ ” notation of eqs 1–3, as it is no longer clear that there are any Si–Si back-bonds. (Most likely there is no more than one, often strained, Si–Si back-bond for each in-surface silicon atom of the copper-containing surfaces.) Process 5 could occur at a temperature lower than for process 4 because an extra enthalpy can come from the transfer of Cl from Cu to Si. (A Cl–Si bond energy is larger than that of Cl–Cu by ~ 20 kcal/mol.)²⁴

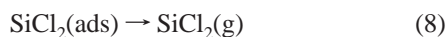
The formation mechanisms of the final desorption products from SiCl_2^* can include the following processes:



Both processes 6 and 7 should be activated at the temperatures below 200°C in order to proceed simultaneously during desorption.

One important question arises from eq 6: why does SiCl_2 desorb at such low temperatures when the barrier for the direct desorption of SiCl_2 from Si(100) was estimated as 3.2 eV³³ and the corresponding TPD peak is observed only at $T > 600^\circ\text{C}$? In answer, the SiCl_2^* can be back-bound to Cu atoms exclusively, since the majority of the Si atoms on the surface are chlorinated and not available for bond formation. From the literature the energy of Si–Cu bonds are approximately 31 kcal/mol³⁴ and the energy of a Si–Si bond is 76 kcal/mol.²⁴ The weaker Si–Cu bond may therefore be the dominating factor in facilitating $\text{SiCl}_2(\text{g})$ desorption from the SiCl_2^* state.

Also pertinent to the question of the SiCl_2 desorption is the hybridization state of the molecular and intermediate SiCl_2^* species. We are suggesting that the direct desorption process



does not occur at either 200°C , I, or 300°C , II. Yet we propose that



is thermally activated at 300°C , II, on the copper-containing surfaces. As the initial and final states of eqs 8 and 9 are

identical, we need to compare directly the activation barriers—that for eq 8 being less than for eq 9. The process of eq 8 could represent a sequential process of back-bond breakages and a removal of sp^3 hybridization of a tetravalent surface bound species. (As the s–p gap of period 3 elements is comparatively large (cf. Si and C), $\text{SiCl}_2(\text{g})$ species shows no hybridization.) We suggest that the copper-containing surfaces allow the formation of a SiCl_2^* species, with a contribution of hybridization removal before complete removal of all back-bonding, thereby reducing the overall activation for SiCl_2 desorption, i.e., the silicon atom in the SiCl_2^* intermediate species is not in a hybridized state. Of note: a similar proposition has been made about a CH_3SiCl surface intermediate of the Direct Synthesis,³⁴ above a copper-containing silicide surface.

Our model therefore predicts that peak I ceases when all $\text{CuCl}(\text{ads})$ species are consumed, and the end of peak II corresponds to the removal of all $\text{SiCl}_2(\text{ads})$ species. (N.B., we cannot say if SiCl_2^* is a mobile species; its mobility is not required for $\text{SiCl}_2(\text{ads})$ depletion, as processes 4 and 6 are both thermally activated.) Also, the model assumes the absence of stable $\text{SiCl}_3(\text{ads})$ species. XPS studies of Si oxidation states and FTIR studies of Cl coordination (shortly underway) will test these consequences of this model.

This work was, in part, motivated by our aim to develop a fuller understanding of the Direct Synthesis, which is described briefly in the Introduction. Under the conditions of the Direct Synthesis ($T \sim 300^\circ\text{C}$, $P_{\text{MeCl}} \sim 1$ atm) one might observe analogous reactions corresponding to our proposed mechanisms for both peaks I and II. Our model is that low-temperature $\text{SiCl}_2(\text{g})$ and $\text{SiCl}_4(\text{g})$ formation proceeds through the surface activated SiCl_2 intermediate. This is fully consistent with the proposals of Lewis, Falconer and co-workers;³⁴ the intermediacy of the surface silylenes CH_3SiCl and SiCl_2 in the Direct Synthesis of methylchlorosilanes. In their and other studies CH_3SiCl and SiCl_2 were not observed in the gas phase.³⁵ This presents no conflict as, if the silylenes do desorb (not considered in³⁴ although suggested in our study), then $\text{CH}_3\text{SiCl}(\text{g})$ and $\text{SiCl}_2(\text{g})$ would presumably react readily with $\text{CH}_3\text{Cl}(\text{g})$ in the high-pressure gas phase to form $(\text{CH}_3)_2\text{SiCl}_2(\text{g})$ and $\text{CH}_3\text{SiCl}_3(\text{g})$.

4. Summary

We have investigated the room-temperature adsorption of chlorine on Si(111) 7×7 and Cu/Si(111) surfaces, and the subsequent thermal desorption of chlorosilanes from these surfaces. The adsorption of chlorine on the Si(111) 7×7 surface followed simple Langmuir kinetics. The adsorption of chlorine on the Cu/Si(111) surfaces proceeds through a mobile precursor, just as expected for adsorption on copper surfaces. The majority of chlorosilane desorption from chlorine exposed Si(111) 7×7 occurred at 650°C (SiCl_2). Desorption peaks at $\sim 600^\circ\text{C}$, consisting of also only SiCl_2 , were observed from the Cu/Si surfaces, but the mechanism of the desorption differs from that of Si(111) 7×7 surface. The presence of Cu on the Si(111) surface enables two lower-temperature pathways for chlorosilane desorption, at 200°C and 300°C . Both lower temperature desorption peaks from the Cu/Si surfaces consisted of mixtures of SiCl_2 and SiCl_4 . We have proposed desorption mechanisms that invoke a single more-loosely bound SiCl_2^* surface intermediate in common to both of the lower temperature desorption peaks.

Acknowledgment. The authors thank T. E. Madey and B. V. Yakshinskyi for helpful discussions and gratefully acknowl-

edge financial support from NSF CHE9732798 and from Dow Corning Corporation for this research.

References and Notes

- (1) Rochow, E. G. *J. Am. Chem. Soc.* **1945**, *67*, 963.
- (2) Yilmaz, S.; Floquet, N.; Falconer, J. L. *J. Catal.* **1996**, *159*, 31.
- (3) Sun, D. H.; Bent, B. E.; Wright, A. P.; Naasz, B. M. *Catal. Lett.* **1997**, *46*, 127.
- (4) Han, J.; Gheysa, S. I.; Strongin, R. D.; Hinch, B. J.; Wright, A. P. *Catal. Lett.* **2000**, *68*, 147.
- (5) Gheysa, S. I.; Strable, B. L.; Strongin, D. R.; Wright, A. P. *Surf. Sci.* **2001**, *474*, 129.
- (6) Kemmann, H.; Muller, F.; Neddermeyer, H. *Surf. Sci.* **1987**, *192*, 11.
- (7) Zegenhagen, J.; Fontes, E.; Grey, F.; Patel, J. R. *Phys. Rev. B* **1992**, *46*, 1860.
- (8) DeSantis, M.; Muntwiler, M.; Osterwalder, J.; Rossi, G.; Sirotti, F.; Stuck, A.; Schlapbach, L. *Surf. Sci.* **2001**, *477*, 179.
- (9) Bootsma, T. I. M.; Hibma, T. *Surf. Sci.* **1995**, *331–333*, 636.
- (10) Daugy, E.; Mathiez, P.; Salvan, F.; Layet, J. M. *Surf. Sci.* **1985**, *154*, 267.
- (11) Kramer, H. M.; Bauer, E. *Surf. Sci.* **1981**, *107*, 1.
- (12) El'tsov, K. N.; Zueva, G. Y.; Klimov, A. N.; Martynov, V. V.; Prokhorov, A. M. *Surf. Sci.* **1991**, *251/252*, 753.
- (13) Gupta, P.; Coon, P. A.; Koehler, B. G.; George, S. M. *Surf. Sci.* **1991**, *249*, 92.
- (14) Whitman, L. J.; Joyce, S. A.; Yarmoff, J. A.; McFeely, F. R.; Terminello, L. J. *Surf. Sci.* **1990**, *232*, 297.
- (15) Durbin, T. D.; Simpson, W. C.; Chakarian, V.; Shuh, D. K.; Varekamp, P. R.; Lo, C. W.; Yarmoff, J. A. *Surf. Sci.* **1994**, *316*, 257.
- (16) Davis, L. I.; McDonald, N. C.; Palmberg, P. W.; Reach, G. E.; Weber, R. E. *Handbook of Auger electron spectroscopy*; Physical Electronics Industries, Inc.: Minnesota, 1976.
- (17) Boland, J. J.; Villarrubia, J. S. *Phys. Rev. B* **1990**, *41*, 9865.
- (18) Gupta, P.; Coon, P. A.; Koehler, B. G.; George, S. M. *J. Chem. Phys.* **1990**, *93*, 2827.
- (19) Nakakura, C. Y.; Phanse, V. M.; Altman, E. I. *Surf. Sci.* **1997**, *370*, L149.
- (20) Winters, H. F. *J. Vac. Sci. Technol. A* **1985**, *3*, 786.
- (21) Masel, R. I. *Principles of adsorption and reaction on solid surfaces*, 1st. ed.; John Wiley & Sons: New York, 1996.
- (22) Matsuo, J.; Yannick, F.; Karahashi, K. *Surf. Sci.* **1993**, *283*, 52.
- (23) Goddard, P. J.; Lambert, R. M. *Surf. Sci.* **1977**, *67*, 180.
- (24) *CRC Handbook of Chemistry and Physics*; Weast, R. C., Ed.; The Chemical Rubber Co.: Cleveland, OH, 1971.
- (25) Szabo, A.; Engel, T. *J. Vac. Sci. Technol. A* **1994**, *12*, 648.
- (26) Dohnalek, Z.; Nishino, H.; Kamoshida, N.; Yates, J. T. *J. Chem. Phys.* **1999**, *110*, 4009.
- (27) Schnell, R. D.; Rieger, D.; Bogen, A.; Himpsel, F. J.; Wandelt, K.; Steinmann, W. *Phys. Rev. B* **1985**, *32*, 8057.
- (28) Miller, J. B.; Siddiqui, H. R.; Gates, S. M.; Russel, J. N.; Yates, J. T.; Tully, J. C.; Cardillo, M. J. *J. Chem. Phys.* **1987**, *87*, 6725.
- (29) Redhead, P. A. *Vacuum* **1962**, *12*, 203.
- (30) Szabo, A.; Farral, P. D.; Engel, T. *Surf. Sci.* **1994**, *312*, 284.
- (31) Chase, M. W., Jr. *NIST-JANAF Thermochemical Tables*, 4th ed.; J. Phys. Chem. Ref. Data, 1998; Vol. 9.
- (32) Jackman, R. B.; Ebert, H.; Foord, J. S. *Surf. Sci.* **1986**, *176*, 183.
- (33) Wijs, G. A. d.; Vita, A. D.; Selloni, A. *Phys. Rev. Lett.* **1997**, *78*, 4877.
- (34) Lewis, K. M.; McLeod, D.; Kanner, B.; Falconer, J. L.; Frank, T. Surface-chemical studies of the mechanism of the Direct Synthesis of methylchlorosilanes. In *Catalyzed Direct Reactions of Silicon*; Lewis, K. M., Rethwisch, D. G., Eds.; Elsevier Science Publishers B. V., 1993.
- (35) Rethwisch, D. G.; Wessel, T. J. Kinetics of the Direct Reaction: mechanistic implications. In *Silicon for Chemical Industry III*; Oye, H. A., Rong, H. M., Ceccaroli, B., Nygaard, L., Tuset, J. K., Eds.; Trondheim: Sandefjord, Norway, 1996; pp 259–268.